Theoretical Study of the Absorption Spectrum and the Thermochemistry of the CF_3OSO_3 Radical

Carlos J. Cobos and Adela E. Croce

Instituto de Investigaciones Fisicoquímicas Teóricas y Aplicadas (INIFTA), Departamento de Química, Facultad de Ciencias Exactas, Universidad Nacional de La Plata, CCT La Plata-CONICET, Casilla de Correo 16, Sucursal 4, (1900) La Plata, Argentina

Reprint requests to A. E. C.; E-mail: acroce@inifta.unlp.edu.ar

The UV-visible absorption spectrum of the recently reported CF_3OSO_3 radical has been studied by using the time-dependent generalization of the density functional theory (TDDFT). For this a set of eleven hybrid functionals combined with the 6-311+G(3df) basis set were employed. The main features of the three experimental absorption bands of CF_3OSO_3 recorded over the 220–530 nm range are well reproduced by the calculations. A dissociation enthalpy for the CF_3O-SO_3 bond of 19.1 kcal mol^{-1} is predicted at the BAC-G3MP2//B3LYP/6-311+G(3df) level of theory.

Key words: CF_3OSO_3; Absorption Spectra; Bond Dissociation Energy; Time-Dependent Density Functional Theory

1. Introduction

Spectroscopic and theoretical studies of the novel CF_3OSO_3 radical have been recently reported [1]. The IR and UV-visible spectra recorded in cryogenic matrices combined with density functional theory (DFT) calculations have provided a conclusive proof for the existence of this species. The absorption spectrum exhibits a strongly structured main band situated between the origin, located at 526.8 nm and 390 nm, and two additional weaker UV bands picked at 305 and 238 nm. The first band resembles in shape the well-known visible band of the related FSO_3 radical [2–6], while the other bands appear to support the new intense band of 275 nm recently reported for FSO_3 [6]. As in this last study, a detailed TDDFT analysis of the UV and visible CF_3OSO_3 spectra (220–530 nm) has been performed in this work. In addition, the CF_3OSO_3 thermal stability has been explored by using high-level ab initio quantum chemical calculations.

2. Computational Methods

The TDDFT theory stands as a promising alternative to cumbersome many-body approaches to the calculation of the electronic excitation [7]. This approach has emerged as a very successful framework to reproduce remarkably well experimental transition energies of valence excited states which can be described by combinations of single one electron transitions [8]. In particular, the TDDFT gives a well-balanced description of open-shell systems such as excited states of radicals [9]. However, the real exchange-correlation functional is unknown and the best DFT model is difficult to establish a priori [10]. For this reason, different formulations are usually employed and tested against experiments. Here, the hybrid functionals B3P86, B3PW91, B3LYP, B1B95, B1LYP, mPW0, B98, B97-1, B97-2, PBE0, and X3LYP as implemented in the Gaussian 03 program package were employed [11]. The large 6-311+G(3df) triple split valence basis set was employed in all cases. The 81 valence electrons of CF_3OSO_3 were accommodated in molecular orbitals which comprise 359 basis functions employing 536 primitive Gaussians. Geometry optimizations without symmetry constraints were carried out using analytical gradient methods. For all DFT methods, real vibrational frequencies were obtained assuring that computed structures correspond to stable compounds. To cover the experimental spectrum, the first eleven electronic states of CF_3OSO_3 were calculated.

3. Absorption Spectra of CF_3OSO_3

Table 1 shows the calculated vertical excitation energies E and oscillator strengths f for the eight more

Table 1. Vertical excitation energies (in eV) and oscillator strengths for the more significant electronic states of CF_3OSO_3 calculated using different functionals with the 6-311+G(3df) basis set.

Level of theory	Property	State							
		1	2	3	4	5	6	7	8
B3P86	E	2.56	2.74	2.77	3.40	4.23	4.99	5.13	5.75
	f	0.0136	0.0227	0.0039	0.0043	0.0047	0.0039	0.0042	0.0131
B3PW91	E	2.591	2.78	2.88	3.49	4.32	5.08	5.22	5.83
	f	0.0117	0.0184	0.0111	0.0037	0.0042	0.0032	0.0035	0.0105
B3LYP	E	2.56	2.74	2.84	3.43	4.26	5.03	5.17	5.76
	f	0.0120	0.0152	0.0141	0.0034	0.0041	0.0031	0.0051	0.0111
B1B95	E	2.56	2.77	2.92	3.62	4.49	5.26	5.46	5.95
	f	0.0108	0.0161	0.0125	0.0046	0.0061	0.0047	0.0085	0.0104
B1LYP	E	2.65	2.79	3.09	3.83	4.21	5.51	5.68	6.16
	f	0.0128	0.0272	0.0053	0.0036	0.0058	0.0043	0.0107	0.0094
mPW0	E	2.71	2.86	3.18	3.93	4.80	5.58	5.76	6.26
	f	0.0127	0.0276	0.0052	0.0039	0.0062	0.0043	0.0110	0.0099
B98	E	2.59	2.78	2.91	3.58	4.43	5.22	5.37	5.92
	f	0.0120	0.0207	0.0097	0.0038	0.0051	0.0039	0.0066	0.0113
B97-1	E	2.57	2.76	2.86	3.49	4.33	5.10	5.24	5.83
	f	0.0118	0.0148	0.0145	0.0037	0.0045	0.0033	0.0054	0.0110
B97-2	E	2.61	2.79	2.93	3.57	4.41	5.18	5.32	5.91
	f	0.0114	0.0183	0.0119	0.0038	0.0047	0.0033	0.0059	0.0105
PBE0	E	2.70	2.86	3.16	3.90	4.77	5.55	5.74	6.24
	f	0.0122	0.0272	0.0055	0.0039	0.0060	0.0042	0.0106	0.0098
X3LYP	E	2.58	2.76	2.89	3.55	4.39	5.18	5.33	5.87
	f	0.0122	0.0223	0.0080	0.0035	0.0047	0.0038	0.0065	0.0114

relevant doublet-doublet valence electronic transitions of CF_3OSO_3. The oscillator strength depends on electronic, Frank-Condon, and spin factors, which reduce the unity maximum value expected for a totally allowed transition, and provides information on the intensity of the experimental band. In spite of the different combinations of exchange and correlation functionals a similar trend is observed. Thus, no approach can be definitely attributed superior to the rest. For this reason, to compare with experiments, the computed data listed in Table 1 were averaged. In this way, the resulting values for E are 2.61 ± 0.05, 2.78 ± 0.04, 2.95 ± 0.13, 3.62 ± 0.19, 4.42 ± 0.20, 5.24 ± 0.21, 5.40 ± 0.23, and 5.95 ± 0.18 eV, while the associated f values are 0.0121 ± 0.0007, 0.0210 ± 0.0049, 0.0092 ± 0.0039, 0.0038 ± 0.0003, 0.0051 ± 0.0008, 0.0038 ± 0.0005, 0.0071 ± 0.0027, and 0.0108 ± 0.0010. It can be observed that the estimated standard deviations are small for E, $1-5\%$, and significantly larger for f, $6-40\%$. The stated limits for E are similar to those derived for the FSO_3 radical, while the deviations are much larger for f, due to the fact that the respective values are smaller [6]. An analysis in terms of the individual DFT methods shows that the B98 method gives the best match to the average values. In fact, this functional leads to deviations of only 0.02 eV and 0.0002 units from the above E and f values. The calculated

excitation energies of 2.61, 2.78 and 2.95 eV lie within the strongest experimental band localized between 2.3 and 3.2 eV. The values of 3.62 and 4.42 eV correspond to the weakest observed band centered at 4.1 eV, while the transitions located at 5.24 and 5.40 eV correspond to the measured band of 5.2 eV.

In order to perform a better comparison between the experiments and the theoretical predictions, a modelling of the spectrum was carried out. To this end, the absorption coefficient of each electronic transition was represented by individual Gaussian functions: $\varepsilon_i = \varepsilon_{max,i} \exp[-(1/2\sigma_i^2)(E_i - E_{max,i})^2]$. Following a procedure similar to that described in [6], the decadic absorption coefficient ε was derived by relating the maximum absorption coefficient ε_{max} with f and with the full width σ of the band at $1/e$ height:

$$\varepsilon \simeq 1.15 \times 10^4 \sum_{i=1}^{\infty} (f_i/\sigma_i) \exp[-(1/2\sigma_i^2)(E_i - E_{max,i})^2].$$

(1)

This expression allows to obtain ε (in M^{-1} cm^{-1}) as a function of the calculated E_i and f_i values. In the absence of a theoretical basis, as frequently, σ was used as a fitted parameter.

Due to the fact that the CF_3OSO_3 concentration and the matrix thickness (the optical pathway) are un-
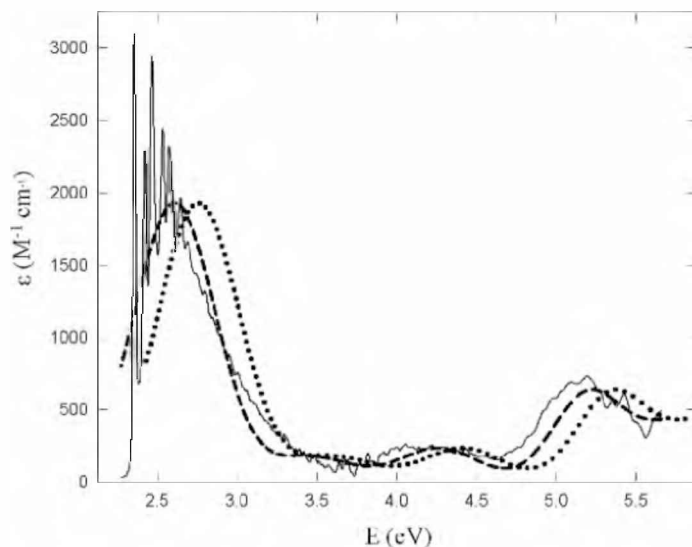
Fig. 1. Comparison between the experimental and computed UV-visible spectra of CF_3OSO_3. (–): [1]; (···): TDDFT calculations (see text); (- - -): TDDFT calculations shifted by -0.15 eV (see text).

known, the spectrum has been reported in absorbance units [1]. For comparison with the theoretical predictions, the absorbance values were appropriately scaled to transform to absorption coefficients ε. Figure 1 shows the spectra obtained by dividing the experimental absorption data by the factor 1.31×10^{-4} M cm, together with the spectrum computed using (1) with the above given set of average E and f values and a single value of $\sigma = 0.21$ eV (i. e. assuming a unique decay rate constant for all of the excited states involved). Even though the whole shape of the spectrum is reproduced, it is clear that the energies of the electronic transitions are somewhat overestimated. By contrast, similar TDDFT calculations lead to a very good agreement in position (470 nm) and intensity (as indicated by the very similar experimental and computed f values) for the strongest absorption band (^2E-X^2A_2) of the FSO_3 radical in the gas phase [6]. In order to match the experimental and theoretical UV band of CF_3OSO_3, all excitation energies were equally shifted by -0.15 eV, as usual in IR spectroscopy. It should be noted that typical TD-B3LYP deviations for excitation energies lie normally within $0.3-0.4$ eV with respect to experiments [12]. This correction implies a red-shift of the theoretical visible band by about 25 nm and of the UV bands by about 8 nm. As Figure 1 shows, the present calculations reproduce reasonably well the global contour of the visible and UV bands. As before, we used $\sigma = 0.21$ eV and a scaling factor for the experimental data of 1.31×10^{-4} M cm. A better agreement between experiments and theory could be clearly ex-

pected employing different σ values for the different transitions. However, no significant improvement was observed by using in (1) the fitted σ values of 0.22 (for transitions $i = 1-3$), 0.25 (for $i = 4,5$), 0.20 (for $i = 6,7$), and 0.29 eV (for $i = 8$), and a scaling constant of 1.34×10^{-4} M cm.

The present simulations allow to transform the experimental CF_3OSO_3 absorbance data on an absolute basis. In this way, the absorption coefficients estimated from the experimental data at about the center of the first band of 480 nm (2.58 eV) and at the band maxima of 305 nm (4.07 eV) and 238 nm (5.21 eV) [1] are 2180, 240, and 690 M^{-1} cm^{-1}, respectively. The first ε value is a factor of two larger than the estimated for CF_3OSO_3 in [1]. In addition, it is also significantly larger than the one measured for FSO_3 at the center of the band located near 470 nm of 1160 M^{-1} cm^{-1} [5].

4. Thermochemistry of CF_3OSO_3

The knowledge of the energetic changes associated with molecular bonds making and breaking is of crucial importance in many practical fields such as atmospheric and combustion chemistry [13–14]. As a first guess, we derived the dissociation enthalpy for the CF_3O-SO_3 bond from the computed total energies (corrected by thermal contributions) of CF_3OSO_3, CF_3O, and SO_3 molecules. The value obtained for this weakest CF_3OSO_3 bond at the composite G3MP2//B3LYP/6-311+G(3df) ab initio level is $\Delta H_{298} = 14.6$ kcal mol^{-1} [15].

Further calculations based on a computed G3MP2//B3LYP/6-311+G(3df) standard enthalpy of formation for CF_3OSO_3 at 298 K corrected by bond additivity [16] were performed. These bond additivity corrections (BAC) account for systematic errors due to deficiencies in the treatment of the interaction electron correlation, molecular electronic structure, and electron pairing. These corrections reduce the estimated G3MP2//B3LYP/6-311+G(3df) enthalpy of formation of -258.4 kcal mol^{-1} to the BAC-G3MP2//B3LYP/6-311+G(3df) value of -265.5 kcal mol^{-1}. Using this last value combined with recommended enthalpies of formation for CF_3O and SO_3 of -151.8 ± 1.7 and -94.62 ± 0.17 kcal mol^{-1} [12] leads to an enthalpy change of $\Delta H_{298} = 19.1 \pm 2$ kcal mol^{-1} for the $CF_3OSO_3 \rightarrow CF_3O + SO_3$ process. The stated errors account for both, experimental and theoretical uncertainties [13, 15, 16]. This enthalpy change is higher than the lower limit computed at the B3LYP/6-311+G(3df) level of 16.7 kcal mol^{-1} and supports the stability predicted for the CF_3OSO_3 radical [1].

5. Conclusion

The present theoretical study indicates that the TDDFT methods are able to explain reasonably well the features of the UV-visible spectrum of CF_3OSO_3. This fact in combination with the here confirmed thermal stability towards the dissociation to CF_3O and SO_3 radicals reinforces the existence of this interesting species, and supports the suggested potential participation of this species in the atmospheric chemistry mechanisms.

[1] S. von Ahsen and J. S. Francisco, J. Phys. Chem. A, **109**, 9193 (2005).

[2] E. Castellano, R. Gatti, J. E. Sicre, and H. J. Schumacher, Z. Phys. Chem. NF, **42**, 174 (1964).

[3] G. W. King, D. P. Santry, and C. H. Warren, J. Mol. Spectrosc. **32**, 108 (1969).

[4] A. E. Croce, J. Photochem. Photobiol. A: Chem. **51**, 293 (1990).

[5] C. J. Cobos, A. E. Croce, and E. Castellano, J. Photochem. Photobiol. A: Chem. **84**, 101 (1994).

[6] C. J. Cobos and A. E. Croce, Z. Phys. Chem. **321**, 897 (2007).

[7] G. Onida, L. Reining, and A. Rubio, Rev. Mod. Phys. **74**, 601 (2002).

[8] K. B. Wiberg, R. E. Stratman, and M. J. Frisch, Chem. Phys. Lett. **297**, 60 (1998).

[9] S. Hirata and M. Head-Gordon, Chem. Phys. Lett. **302**, 375 (1999).

[10] P. Hohenberg and W. Kohn, Phys. Rev. B, **136**, 864 (1964).

[11] Gaussian 03, Revision D.01, M. J. Frisch, G. W. Trucks, H. B. Schlegel, G. E. Scuseria, M. A. Robb, J. R. Cheeseman, J. A. Montgomery, Jr., T. Vreven, K. N. Kudin, J. C. Burant, J. M. Millam, S. S. Iyengar, J. Tomasi, V. Barone, B. Mennucci, M. Cossi, G. Scalmani, N. Rega, G. A. Petersson, H. Nakatsuji, M. Hada, M. Ehara, K. Toyota, R. Fukuda, J. Hasegawa, M. Ishida, T. Nakajima, Y. Honda, O. Kitao, H. Nakai, M. Klene, X. Li, J. E. Knox, H. P. Hratchian, J. B. Cross, V. Bakken, C. Adamo, J. Jaramillo, R. Gomperts, R. E. Stratmann, O. Yazyev, A. J. Austin, R. Cammi, C. Pomelli, J. W. Ochterski, P. Y. Ayala, K. Morokuma, G. A. Voth, P. Salvador, J. J. Dannenberg, V. G. Zakrzewski, S. Dapprich, A. D. Daniels, M. C. Strain, O. Farkas, D. K. Malick, A. D. Rabuck, K. Raghavachari, J. B. Foresman, J. V. Ortiz, Q. Cui, A. G. Baboul, S. Clifford, J. Cioslowski, B. B. Stefanov, G. Liu, A. Liashenko, P. Piskorz, I. Komaromi, R. L. Martin, D. J. Fox, T. Keith, M. A. Al-Laham, C. Y. Peng, A. Nanayakkara, M. Challacombe, P. M. W. Gill, B. Johnson, W. Chen, M. W. Wong, C. Gonzalez, J. A. Pople, Gaussian, Inc., Wallingford CT, 2004.

[12] S. Grimme, in: Reviews on Computational Chemistry (Eds. K. B. Lipkowitz, R. Larter, T. R. Cundari), Wiley-VCH, John Wiley & Sons, Inc., Volume 20, 2004, p. 153.

[13] S. P. Sander, R. R. Friedl, D. M. Golden, M. J. Kurylo, G. K. Moortgat, P. H. Wine, A. R. Ravishankara, C. E. Kolb, M. J. Molina, B. J. Finlayson-Pitts, R. E. Huie, V. L. Orkin, Chemical Kinetics and Photochemical Data for Use in Atmospheric Studies; NASA/JPL Data Evaluation, JPL Publication 06-2 Evaluation No. 15; NASA: Pasadena, CA, November 20, 2006. http://jpldataeval.jpl.nasa.gov/¡/a¿.

[14] D. L. Baulch, C. T. Bowman, C. J. Cobos, R. A. Cox, Th. Just, J. A. Kerr, M. J. Pilling, D. Stocker, J. Troe, W. Tsang, J. Walker, and J. Warnatz, J. Phys. Chem. Ref. Data, **34**, 757 (2005).

[15] A. G. Baboul, L. A. Curtiss, and P. C. Redfern, J. Chem. Phys. **110**, 7650 (1999).

[16] B. Anantharaman and C. F. Melius, J. Phys. Chem. A, **109**, 1734 (2005).